Nanoscale

RSC Publishing

PAPER

View Article Online
View Journal | View Issue

Cite this: *Nanoscale*, 2013, **5**, 4855

Single-molecule analysis of the major glycopolymers of pathogenic and non-pathogenic yeast cells

Sofiane El-Kirat-Chatel,†‡[a] Audrey Beaussart,†‡[a] David Alsteens,†‡[a] Aurore Sarazin,†‡[b] Thierry Jouault†[b] and Yves F. Dufrêne†*[a]

Received 15th February 2013
Accepted 29th March 2013

DOI: 10.1039/c3nr00813d

www.rsc.org/nanoscale

Most microbes are coated with carbohydrates that show remarkable structural variability and play a crucial role in mediating microbial–host interactions. Understanding the functions of cell wall glycoconjugates requires detailed knowledge of their molecular organization, diversity and heterogeneity. Here we use atomic force microscopy (AFM) with tips bearing specific probes (lectins, antibodies) to analyze the major glycopolymers of pathogenic and non-pathogenic yeast cells at molecular resolution. We show that non-ubiquitous β-1,2-mannans are largely exposed on the surface of native cells from pathogenic *Candida albicans* and *C. glabrata*, the former species displaying the highest glycopolymer density and extensions. We also find that chitin, a major component of the inner layer of the yeast cell wall, is much more abundant in *C. albicans*. These differences in molecular properties, further supported by flow cytometry measurements, may play an important role in strengthening cell wall mechanics and immune interactions. This study demonstrates that single-molecule AFM, combined with immunological and fluorescence methods, is a powerful platform in fungal glycobiology for probing the density, distribution and extension of specific cell wall glycoconjugates. In nanomedicine, we anticipate that this new form of AFM-based nanoglycobiology will contribute to the development of sugar-based drugs, immunotherapeutics, vaccines and diagnostics.

The yeast cell wall is a complex three dimensional structure composed of an inner layer containing chitin and β-glucans, and an outer layer made of α-mannans, mannoproteins and glycolipids (Fig. 1).[1,2] Besides this conserved composition, some yeast species have additional compounds and structures, such as melanin and capsules for *Cryptococcus neoformans*,[2,3] and β-mannans for *Candida albicans*, *C. glabrata* and *C. lusitaniae*.[2,4–6] Although the chemical composition of the yeast cell wall is well known, how the individual components are spatially organized at the nanoscale remains elusive.

Candida species are opportunistic yeast pathogens responsible for severe infections in immuno-compromised patients.[7,8] During fungal infection, cell wall glycans constitute the main target components (so-called pathogen associated molecular pattern, PAMP) recognized by immune cell receptors (pathogen recognition receptors, PRRs).[7,9] Depending on the types of cell wall components and host receptors, various specific host inflammatory responses can be elicited. Besides common cell wall carbohydrates, non-ubiquitous glycans like β-mannans may also interact with immune cell receptors.[7,10,11] Host receptors are grouped as C-type lectin receptors and Toll-like receptors (TLR) that both recognize mannans, glucans and chitin of the cell wall and subsequently induce pro- or anti-inflammatory responses through cytokine production.[7,11–13] Mannose receptors recognize

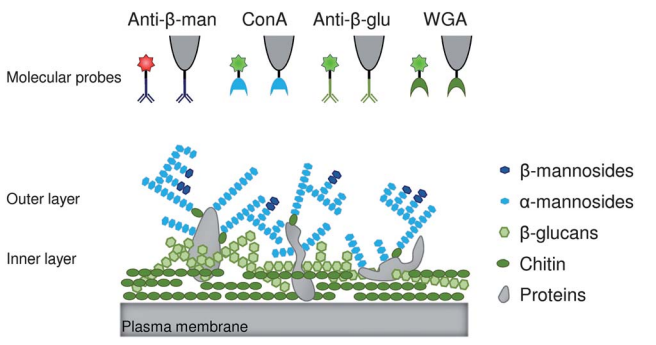

Fig. 1 Use of single-molecule AFM and fluorescence methods for probing the density, distribution and extension of yeast cell wall glycoconjugates. Schematic representation of the cell wall surrounding the yeast plasma membrane. While the inner cell wall layer contains chitin and β-1,3-glucans, the outer layer contains α-mannans together with β-1,2-mannans for some species. Molecular probes (antibodies, lectins) used for fluorescence staining and AFM detection are also shown.

[a]*Université catholique de Louvain, Institute of Life Sciences, Croix du Sud, 1, bte L7.04.01., B-1348 Louvain-la-Neuve, Belgium. E-mail: Yves.Dufrene@uclouvain.be*

[b]*Inserm U995, équipe 2, Université Lille 2, Faculté de Médecine, Pôle Recherche, 1 Place Verdun, 59045 Lille Cedex, France*

† Yves Dufrêne, Thierry Jouault, Sofiane El-Kirat-Chatel, Audrey Beaussart, David Alsteens and Aurore Sarazin designed the research, analyzed the data and wrote the paper.

‡ Sofiane El-Kirat-Chatel, Aurore Sarazin, Audrey Beaussart and David Alsteens performed the research.

mannans and induce pro-inflammatory response when associated with TLR2.[5,13] Galectin 3, in association with TLR2, recognizes β-1,2-mannose residues and induces pro-inflammatory responses.[10,11,14] Dectin-1 binds β-1,3-glucans and has pro-inflammatory effects.[15–18] Finally, chitin receptors[19,20] may recognize chitin after degradation of the outer cell wall layer and block pro-inflammatory cytokine production by immune cells.[21]

While the interactions between cell wall glycans and immune cells have been widely investigated, how the different glycoconjugates are distributed in space and how this distribution varies from species to species is poorly understood. Traditionally, the yeast cell wall composition is analyzed using bulk techniques like high pressure liquid chromatography,[22] nuclear magnetic resonance,[23] immuno-fluorescence,[4] and/or mass spectrometry.[24] Although powerful, these methods have no/poor spatial resolution, meaning that the nanoscale surface distribution and exposure of various components are not accessible. This information is critical to our understanding of pathogen–immune interactions. Here, we use single-molecule atomic force microscopy (AFM)[25–27] to detect and localize individual cell wall glycans on the surface of pathogenic *C. albicans* and *C. glabrata* and non-pathogenic *Saccharomyces cerevisiae*. Using AFM tips labelled with specific antibodies and lectins (Fig. 1), we probe the surface density, distribution and extension of β-mannans and α-mannans from the outer yeast cell wall layer, and β-glucans and chitin from the inner layer, all of which are critical for immune interactions. Consistent with flow cytometry measurements, the results show substantial differences between pathogenic and non-pathogenic yeasts which we believe are of biological significance. These single-molecule imaging experiments represent an exciting new approach in fungal glycobiology.

Results and discussion

Probing the diversity of cell wall glycans at the population level using flow cytometry

We first investigated the cell wall glycans of *C. albicans* using flow cytometry. Fluorescent labelled (fluorescein isothiocyanate, FITC) lectins and antibodies were used to probe β-mannans, α-mannans, β-glucans and chitin, a polymer of *N*-acetyl-glucosamine (Glc*N*Ac). Fig. 2a shows a plot of the cellular complexity (side scatter, SSC) against the cell size (forward scatter, FSC), revealing a homogenous morphological population. Fig. 2b–f show the number of cells as a function of the fluorescence intensity for each specific dye, *i.e.* FITC and phycoerythrin (PE). Fig. 2b corresponds to the analysis of unstained cells as a negative control to define the fluorescence baseline for FITC and PE. Glycans of the outer cell wall layer were specifically labelled as follows (Fig. 1): β-mannans were probed using anti-β-man (5B2) monoclonal antibodies,[28] followed by a secondary antibody conjugated to PE (Fig. 2c), while α-mannans were probed with the lectin Concanavalin A (ConA) conjugated to FITC (Fig. 2d). For both staining experiments, positive fluorescence events (right peaks) were clearly distinguished from the background fluorescence (left peaks), demonstrating substantial exposure of β-mannans and α-mannans on the outermost surface of *C. albicans*. Inner layer β-glucans and chitin were specifically labelled using anti-β-glu monoclonal antibodies and FITC conjugated secondary antibodies, and FITC–wheat germ agglutinin (WGA) lectins, respectively (Fig. 1). No positive fluorescent cells were detected with these specific probes since the peak corresponding to labelled cells completely overlaid the background fluorescence peak (Fig. 2e and f). This observation confirms that chitin and β-glucan compounds of the inner cell wall layer were not directly accessible.[4,29]

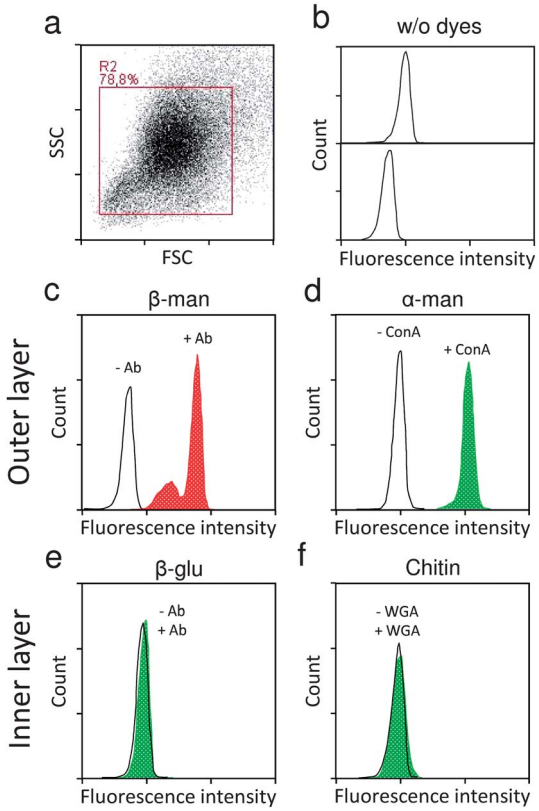

Fig. 2 Detection of *C. albicans* cell wall glycans by flow cytometry. (a) Representation of the *C. albicans* population according to its size (forward scatter, FSC) and its subcellular complexity (side scatter, SSC). (b) Negative control on unstained *C. albicans* cells defining the background fluorescence for fluorescein isothiocyanate (FITC) (top) and phycoerythrin (PE) (bottom). (c) Fluorescence detection of β-1,2-mannans using an anti-β-1,2-mannoside monoclonal antibody and a secondary antibody coupled to PE. (d) α-Mannan detection by cell staining with Concanavalin A (ConA)–FITC. (e and f) Staining of live cells with a β-1,3-glucan monoclonal antibody and a secondary antibody coupled to FITC (e), and with wheat germ agglutinin (WGA)–FITC (f) demonstrates the non-accessibility of β-1,3-glucans and chitin.

Imaging single β-mannans on living yeast cells

We then used AFM recognition imaging to detect and localize individual glycan molecules on different strains, focusing first on non-ubiquitous β-1,2-mannans. These glycans are attached to the terminal position of the acid labile side chain of α-mannans and have been shown to elicit specific immune responses.[2,10,14,30,31] We first observed the surface morphology of the cells using a silicon nitride tip. Representative topographic

images of single *C. albicans*, *C. glabrata* and *S. cerevisiae* cells immobilized in porous membranes are shown in Fig. 3. Using small imaging forces (~100 pN), images were obtained repeatedly without detaching the cell or altering significantly the surface morphology. The cells were smooth and homogeneous (surface roughness of ~1 nm), without substantial differences between the strains.

Spatially resolved force curves were then recorded across the cell surface using AFM tips modified with anti-β-man antibodies. Fig. 4 shows the adhesion (or recognition) maps, adhesion histograms with typical force curves and rupture length histograms obtained on *C. albicans*, *C. glabrata* and *S. cerevisiae*. These single-molecule imaging results clearly document the massive recognition of β-1,2-mannans on *C. albicans* and *C. glabrata*, while these compounds are hardly detected on *S. cerevisiae*. Fig. 4a–c indeed reveal that, on *C. albicans*, a large portion of the force curves (50%) showed binding events. We believe these features reflect the massive detection of individual β-1,2-mannose-rich glycoconjugates for several reasons. First, the mean adhesion force, 41 ± 14 pN (n = 1024), was in the range of the values expected for single antibody–antigen bonds at similar loading rates;[32] second, these signatures were essentially missing in non-pathogenic *S. cerevisiae* which lacks β-mannans (Fig. 4g–i); third, the detection of β-mannans in large amounts on the cell surface, corresponding to a minimum surface density of 512 sites per μm^2, is consistent with the flow cytometry analysis of *C. albicans* cell populations (Fig. 2). Adhesion profiles showed long rupture distances, typically in the ~10 to 500 nm range, indicating that β-mannan-associated macromolecules were long and loosely bound to the cell wall. Interestingly, we found that glycans were not randomly distributed but seemed to be organized into nanoscale network patterns and the surrounding regions lack glycan molecules (Fig. 4a). We suggest this pattern reflects the heterogeneous organization of β-mannans in the yeast cell wall, an interpretation which is supported by fluorescence microscopy images revealing patchy β-mannan distributions in whole cells (Fig. 4a). These nanodomains may induce the recruitment of clustered receptors formed by tetraspanin microdomains within immune cells.[33] Fig. 4d–f show that β-mannan properties of *C. glabrata* were quite similar to those of *C. albicans*, except that the amount of β-1,2-mannosides detected was slightly lower, corresponding to a minimum surface density of 384 sites per μm^2, and that much shorter rupture distances were observed, ~10 to 150 nm, suggesting shorter or more compact molecules.

Taken together, the above observations indicate that β-1,2-mannose-rich glycoconjugates were detected and stretched on the outermost surface of *C. albicans* and *C. glabrata*, thereby explaining their specific interactions with immune cells. These glycopolymers are abundant, seem to be heterogeneously organized, and show differences in density and extensions between the two strains. Whether the higher density and longer extensions found in *C. albicans* may play a role in increasing the immune response remains to be elucidated. These experiments demonstrate that AFM with tips bearing specific antibodies is a valuable method in glycobiology for the single-molecule detection and biophysical analysis of fungal cell wall glycans, thus complementing traditional cell wall characterization techniques.

Single-molecule recognition imaging of α-mannans

Next, we used AFM tips bearing the lectin ConA to probe the distribution and extension of α-mannans, which are ubiquitous components of all fungal cell walls (Fig. 5). Force data collected on *C. albicans* (Fig. 5a–c) documented a large portion of binding events (46%), suggesting that α-mannan chains were highly exposed, a finding consistent with flow cytometry data. The curves showed essentially single adhesion events, along with elongation forces and rupture lengths ranging from 20 to 500 nm. Although the distribution of adhesion forces was broad, most events being in the 40–200 pN range, it was roughly consistent with the presence of two maxima at 46 ± 9 pN and 81 ± 29 pN. As the force of single ConA–mannose interactions is 57 ± 19 pN,[34] the ~46 pN and ~81 pN forces may be attributed to the detection of one and two α-mannan chains. As for β-mannans, adhesion maps suggested that the organization of α-mannans was heterogeneous. A small portion of adhesion signatures showed long rupture distances that were up to 500 nm, thus similar to those measured for β-mannans. This is consistent with structural data showing that β-mannans are attached to terminal α-mannan side chains.[35,36] Hence, we

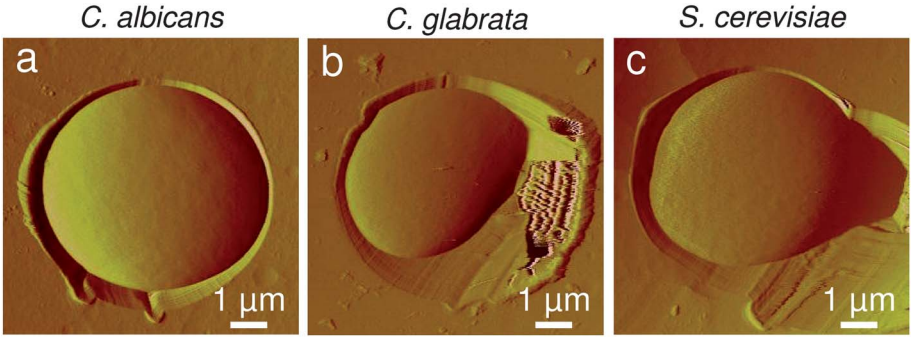

Fig. 3 AFM images of living yeast cells. (a–c) AFM deflection images in buffer of single cells from *Candida albicans* (a), *Candida glabrata* (b) and *Saccharomyces cerevisiae* (c). Similar data were obtained in multiple experiments using different tips and cell cultures.

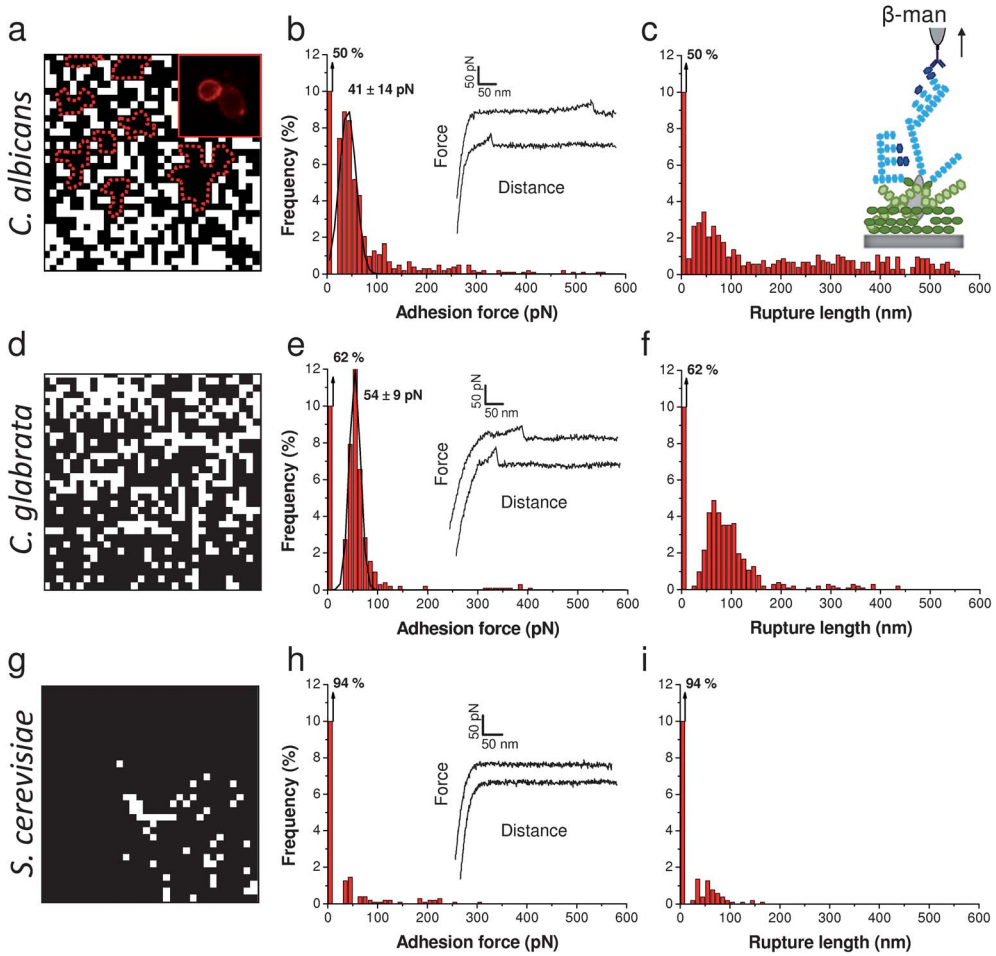

Fig. 4 Molecular mapping of cell surface β-mannans. (a, d and g) Adhesion force maps (1 μm × 1 μm; white pixels correspond to adhesion events, black pixels represent non adhesive events) recorded in buffer between an AFM tip functionalized with an anti-β-1,2-mannoside monoclonal antibody (5B2) and the surface of *C. albicans* (a), *C. glabrata* (d) and *S. cerevisiae* (g). (b, e and h) Corresponding adhesion force histograms ($n = 1024$) together with representative force curves, and (c, f and i) histograms of rupture distances. The inset in (a) shows a fluorescence image of *C. albicans* cells revealing the patchy organization of β-mannans. The dotted lines in (a) emphasize the heterogeneous nanoscale distribution of β-mannans. Similar data were obtained in multiple experiments using different tips and cell cultures.

expect that pulling on β-mannans will also result in stretching α-mannan chains.

C. glabrata and *S. cerevisiae* showed the same level of detection (Fig. 5d–i), consistent with the notion that their cell wall is also rich in α-mannans. Yet, two minor differences were noted, *i.e.* shorter extensions (10–200 nm) as observed for β-mannans, and a slightly broader distribution of adhesion forces for *S. cerevisiae*, suggesting higher surface exposure of α-mannosides. In summary, AFM showed that α-mannans are largely exposed on the surface of the three species, and that some of them exhibit longer extensions on *C. albicans*.

Probing β-glucans and chitin from the inner cell wall

Together with chitin fibrils, β-1,3-glucans are present in the inner layer of the cell wall and are responsible for structural integrity and cell shape.[1,2,24] Evidence is increasing that these glycans may also mediate immune interactions.[5,18–21,37–40] Therefore, a pertinent question is to know whether the polymer properties (density, distribution, extension) of inner and outer layer glycans differ. Consistent with the literature,[4,41] flow cytometry showed that inner layer β-1,3-glucans and chitin are masked by outer layer components, thus not accessible to fluorescence and AFM probes. To address these glycans by AFM, we therefore analyzed yeast cells followed by heat treatment, a procedure known to expose inner cell wall components.[4,29,41,42] Fig. 6 shows the adhesion maps, adhesion histograms with force curves and rupture length histograms obtained for *C. albicans* (Fig. 6a–c), *C. glabrata* (Fig. 6d–f) and *S. cerevisiae* (Fig. 6g–i) cells with AFM tips bearing antibodies directed against β-1,3-glucans. Mean adhesion forces of ~40 pN were observed, consistent with antibody–antigen interactions thus with single β-glucan detection. β-glucans were detected in similar amounts in the three species, and their rupture lengths suggested that they were more extended, thus longer or more flexible on *C. albicans* and *C. glabrata* (up to 200 nm) than on *S. cerevisiae* (up to 100 nm). This difference may account for differences in cell wall nanomechanics.

How about chitin? Fig. 7 shows the force data obtained for the three species with AFM tips bearing WGA lectins. Mean adhesion forces of ~40 to 65 pN were observed, which is in the range of forces expected for the WGA–Glc*N*Ac interaction

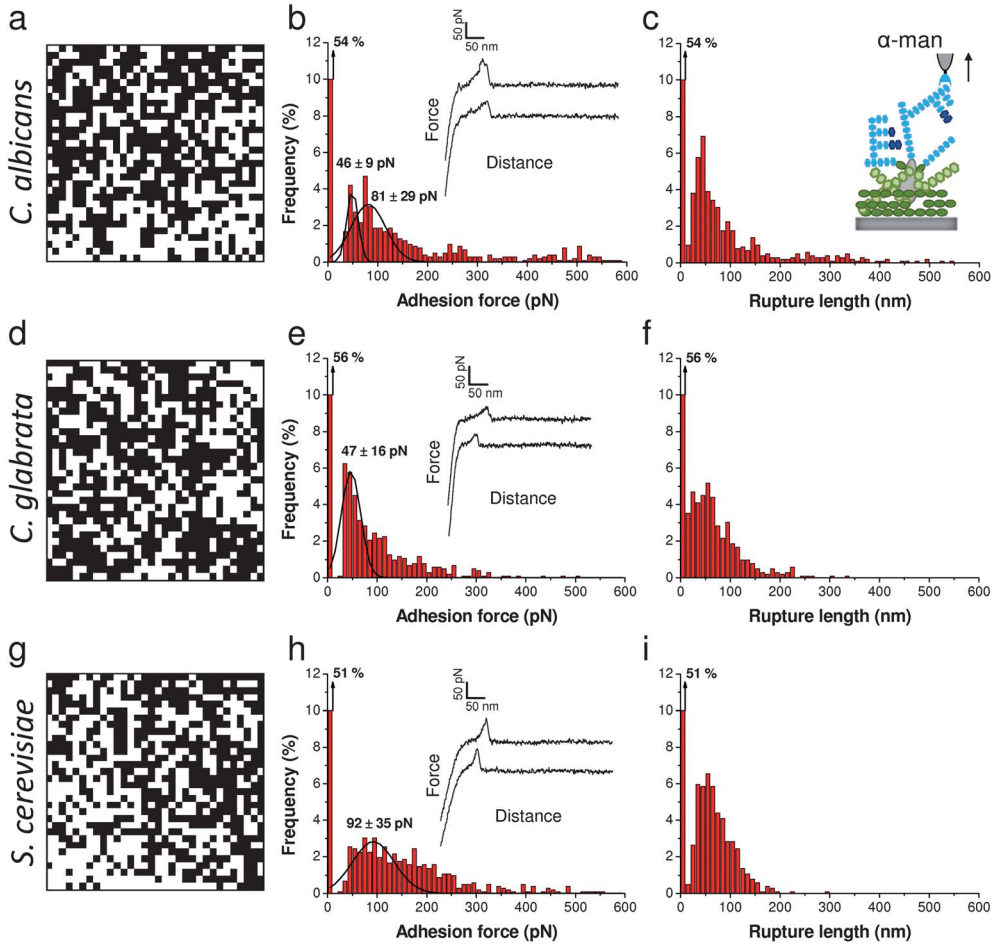

Fig. 5 Molecular mapping of cell surface α-mannans. (a, d and g) Adhesion force maps (1 μm × 1 μm) recorded in buffer between a ConA-tip and the surface of *C. albicans* (a), *C. glabrata* (d) and *S. cerevisiae* (g). (b, e and h) Corresponding adhesion force histograms ($n = 1024$) together with representative force curves, and (c, f and i) histograms of rupture distances. Similar data were obtained in multiple experiments using different tips and cell cultures.

(47 ± 15 pN).[43] Although Glc*N*Ac was detected in the three species, it was more abundant in *C. albicans* than in *C. glabrata* and *S. cerevisiae* (56% *vs.* 26% and 34%, respectively). This suggests that the *C. albicans* cell wall is richer in chitin, which agrees well with previous whole cell chitin quantification revealing that *C. albicans* contains at least twice as much chitin as the two other species.[24] This higher chitin content could have important biological functions by strengthening cell wall mechanics,[1,44,45] providing higher resistance to phagosome stress[46] and enhancing *C. albicans*–immune interactions.[21]

Single-molecule AFM as a new tool in microbial glycobiology

Most living cells are decorated with sugars that often bind to proteins or lipids. Glycopolymers therefore play a crucial role in the interaction between cells and their environment. In fungi, the cell wall is made of a complex mixture of glycans that have distinct functions, including maintaining cell shape and integrity, and binding to receptors like lectins on host cells or other fungal cells. Studying the diversity and heterogeneity of the yeast cell wall glycoconjugates is critical to our understanding of their functions. While traditional techniques provide averaged information on the cell wall composition, they are not surface specific and/or they lack spatial resolution. Our experiments demonstrate that single-molecule AFM, combined with immunological (β-glycan specific antibodies) and fluorescence (flow cytometry) methods, is a powerful platform for probing the density, distribution and extension of yeast glycoconjugates to molecular resolution. The results show substantial differences between pathogenic and non-pathogenic yeasts. Unlike *S. cerevisiae*, *C. albicans* and *C. glabrata* are decorated with large amounts of β-1,2-mannans that seem to have heterogeneous spatial organization. β-1,2-mannans from *C. albicans* show the highest density and longest extensions, a behaviour that may modulate immune responses. *C. albicans* also shows a much higher content of chitin in its inner cell wall layer, which could also play a role in cell wall mechanics and immune interactions.

Methods

Microorganisms, cultures conditions and reagents

C. albicans SC5314, *C. glabrata* ATCC 90030 and *S. cerevisiae* S288C (MUCL 38902) were cultivated in YPD medium (1% yeast extract, 2% Bacto-peptone, 2% D-glucose) at 30 °C and with shaking at 200 rpm. Prior to analysis, yeast cells were always harvested by

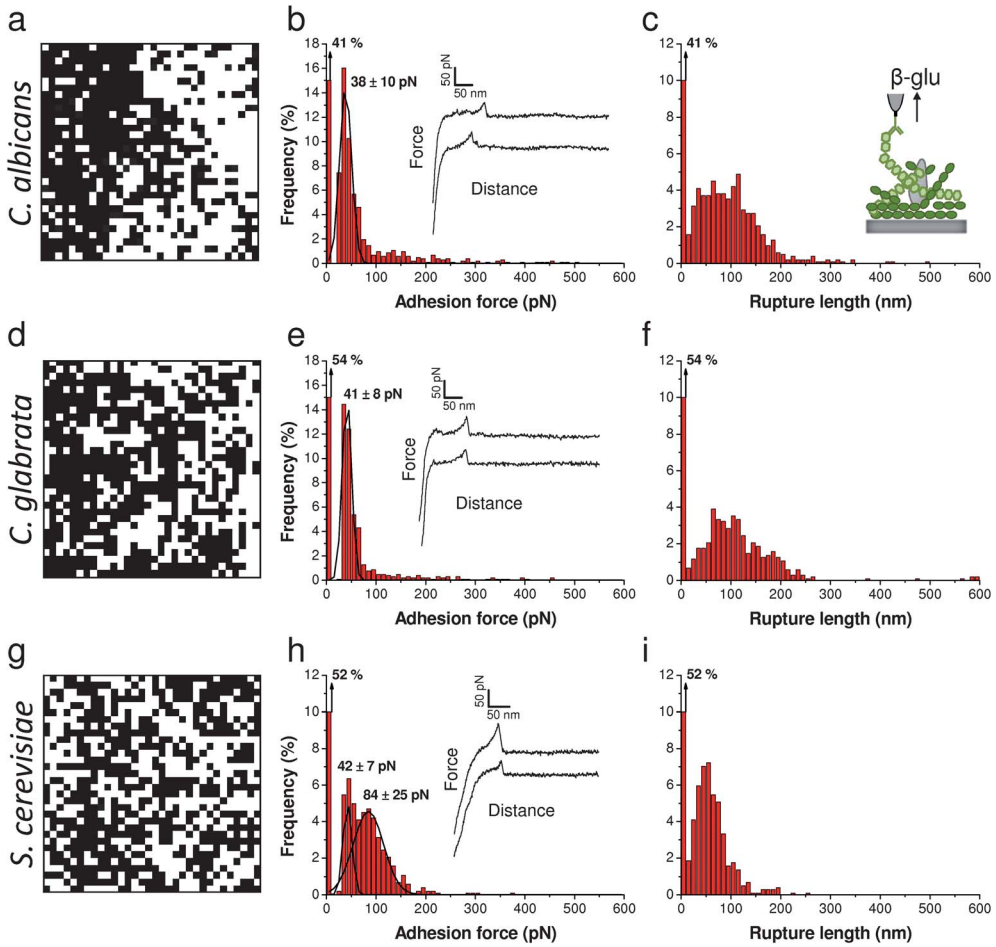

Fig. 6 Imaging β-1,3-glucans from the inner cell wall layer. (a, d and g) Adhesion force maps (1 μm × 1 μm) recorded in buffer between an AFM tip functionalized with an anti-β-1,3-glucans monoclonal antibody and the surface of heat-treated cells from *C. albicans* (a), *C. glabrata* (d) and *S. cerevisiae* (g). (b, e and h) Corresponding adhesion force histograms ($n = 1024$) together with representative force curves, and (c, f and i) histograms of rupture distances. Similar data were obtained in multiple experiments using different tips and cell cultures.

centrifugation, washed 3 times with TBS and resuspended to a concentration of ~1×10^6 cells per ml in 10 ml TBS containing 1 mM $CaCl_2$ and 1 mM $MnCl_2$. To expose the inner cell wall glycans, yeast cells were heat treated at 90 °C for 20 min and then the cells were washed 3 times with TBS prior to analysis.[29]

The anti-β-1,2-mannosides monoclonal antibody 5B2, a rat IgM, was obtained in the laboratory of T.J.[28] Anti-β-1,3-glucans, a mouse monoclonal IgG, was provided by Biosupplies (Pty, Australia). Wheat germ agglutinin (WGA), Concanavalin A (ConA), fluorescein isothiocyanate (FITC) conjugated WGA and biotin-ConA were purchased from Sigma. Phycoerythrin (PE)-, FITC-conjugated anti-rat IgM, anti-mouse IgG or anti-rabbit IgG or streptavidin–FITC were obtained from Southern Biotechnology Laboratories (Birmingham, AL).

Flow cytometry

C. albicans cells (1×10^6) were washed with PBS containing 2% fetal calf serum (PBS–FCS) and then incubated for 15 min with either anti-β-1,2-mannosides (5B2, 8 μg ml^{-1}), or anti-β-1,3-glucans (20 μg ml^{-1}) antibodies or ConA-biotin. After washing, the yeast cells were incubated for 15 min with either specific secondary PE or FITC-labeled antibodies (diluted 1 : 100), WGA–FITC (diluted 1 : 1000) or streptavidin–FITC (1 : 500). A negative control was performed by adding labeled second antibody only, at the same concentration. All processes were carried out at 4 °C in PBS–FCS. After washing, the cells were fixed with 0.4% paraformaldehyde and examined with a fluorescence-activated cell sorter (FACS).

Flow cytometry was performed using an Accuri C6 flow cytometer (BD Biosciences) equipped with an argon ion laser with an excitation power of 15 mW at 488 nm. Forward scatter (FSC) and side scatter (SSC) were analyzed on linear scales, while green (FL1) and red fluorescence intensity (FL2) on logarithmic scales. Analysis gates were set around debris and intact cells on an FSC *versus* SSC dot plot. The fluorescence histograms of 10 000 cells were generated using the gated data. Data acquisition and analysis were performed using CFlow® sampler analysis software.

Atomic force microscopy

AFM measurements were performed at room temperature (20 °C) in TBS containing 1 mM $CaCl_2$ and 1 mM $MnCl_2$ using a

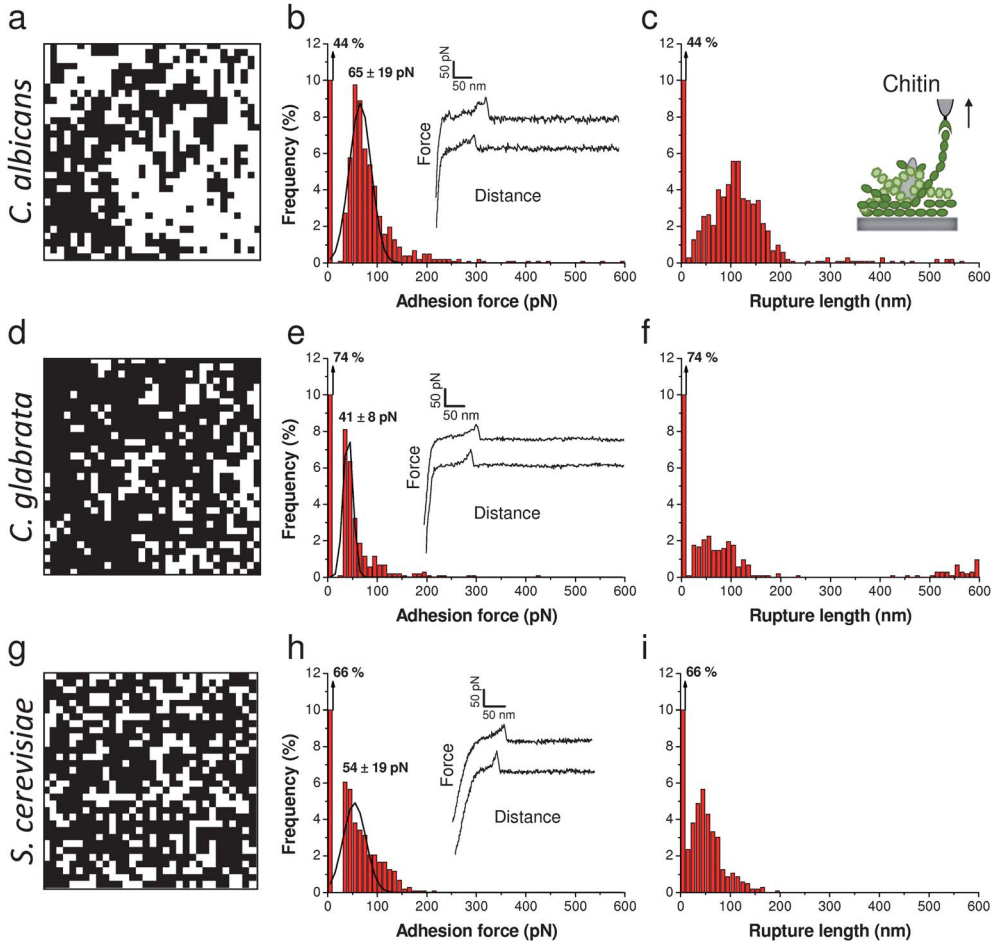

Fig. 7 Imaging chitin from the inner cell wall layer. (a, d and g) Adhesion force maps (1 μm × 1 μm) recorded in buffer between a WGA-tip and the surface of heat-treated cells from *C. albicans* (a), *C. glabrata* (d) and *S. cerevisiae* (g). (b, e and h) Corresponding adhesion force histograms ($n = 1024$) together with representative force curves and (c, f and i) histograms of rupture distances ($n = 1024$) corresponding to the recorded maps. Similar data were obtained in multiple experiments using different tips and cell cultures.

Nanoscope V Multimode AFM (Bruker corporation, Santa Barbara, CA) and oxide sharpened microfabricated Si_3N_4 cantilevers with a nominal spring constant of ~0.01 N m^{-1} (Microlevers, Bruker corporation). Yeast cells were immobilized by mechanical trapping into porous polycarbonate membranes (Millipore, Billerica, MA) with a pore size similar to the cell size.[25,47]

For single-molecule imaging, AFM tips were functionalized with monoclonal antibodies or lectins using PEG–benzaldehyde linkers.[48] Prior to functionalization, cantilevers were washed with chloroform and ethanol, placed in an UV-ozone-cleaner for 30 min, immersed overnight into an ethanolamine solution (3.3 g ethanolamine into 6 ml of DMSO), then washed 3 times with DMSO and 2 times with ethanol, and dried with N_2. The ethanolamine-coated cantilevers were immersed for two hours in a solution prepared by mixing 1 mg acetal-PEG-NHS dissolved in 0.5 ml of chloroform with 10 μl triethylamine, then washed with chloroform and dried with N_2. Cantilevers were further immersed for 10 min in a 1% citric acid solution, washed with Milli-Q water, and then covered with a 200 μl droplet of PBS solution containing the probing proteins (0.2 mg ml^{-1}) to which 2 μl of a 1 M $NaCNBH_3$ solution were added. After 50 min, cantilevers were incubated with 5 μl of a 1 M ethanolamine solution in order to passivate unreacted aldehyde groups, and then washed with and stored in buffer. A single cell was first localized using a bare tip, after which the tip was changed with a functionalized tip. Adhesion maps were obtained by recording 32 × 32 force–distance curves on areas of 1 μm^2, calculating the adhesion force for each force curve and displaying the adhesive event as a white pixel. All force curves were recorded with a maximum applied force of 250 pN, using a constant approach and retraction speed of 1000 nm s^{-1}.

Fluorescence microscopy

After 20 h of culture, yeast cells were plated onto ten-well microscopy slides (10^6 yeast in 50 μl per well) and allowed to dry overnight under a hood at 20 °C. After washing with PBS, the wells were blocked for 20 min with PBS–1% BSA, then incubated with 5B2 antibody (1/50 dilution in PBS–1% BSA) for 1 h and revealed with a 1/50 dilution of PE-conjugated anti-rat IgM for 1 h. Slides were then washed five times and mounted for microscopic examination.

Acknowledgements

Work at the Université catholique de Louvain was supported by the National Foundation for Scientific Research (FNRS), the Université catholique de Louvain (Fonds Spéciaux de Recherche), the Région Wallonne, the Federal Office for Scientific, Technical and Cultural Affairs (Interuniversity Poles of Attraction Programme), and the Research Department of the Communauté française de Belgique (Concerted Research Action). Y.F.D. and D.A. are Senior Research Associate and Postdoctoral Researcher of the FRS-FNRS. T.J. is a Research Associate of Inserm.

References

1 F. M. Klis, A. Boorsma and P. W. J. De Groot, *Yeast*, 2006, **23**, 185.
2 J. Masuoka, *Clin. Microbiol. Rev.*, 2004, **17**, 281.
3 S. Frases, A. Salazar, E. Dadachova and A. Casadevall, *Appl. Environ. Microbiol.*, 2007, **73**, 615.
4 M. Martinez-Esparza, A. Sarazin, N. Jouy, D. Poulain and T. Jouault, *J. Immunol. Methods*, 2006, **314**, 90.
5 M. G. Netea, N. A. Gow, C. A. Munro, S. Bates, C. Collins, G. Ferwerda, R. P. Hobson, G. Bertram, H. B. Hughes, T. Jansen, L. Jacobs, E. T. Buurman, K. Gijzen, D. L. Williams, R. Torensma, A. McKinnon, D. M. MacCallum, F. C. Odds, J. W. Van der Meer, A. J. Brown and B. J. Kullberg, *J. Clin. Invest.*, 2006, **116**, 1642.
6 N. Shibata, H. Kobayashi, Y. Okawa and S. Suzuki, *Eur. J. Biochem.*, 2003, **270**, 2565.
7 M. G. Netea, G. D. Brown, B. J. Kullberg and N. A. Gow, *Nat. Rev. Microbiol.*, 2008, **6**, 67.
8 M. A. Pfaller and D. J. Diekema, *Clin. Microbiol. Rev.*, 2007, **20**, 133.
9 N. A. Gow, F. L. van de Veerdonk, A. J. Brown and M. G. Netea, *Nat. Rev. Microbiol.*, 2012, **10**, 112.
10 T. Jouault, M. El Abed-El Behi, M. Martinez-Esparza, L. Breuilh, P. A. Trinel, M. Chamaillard, F. Trottein and D. Poulain, *J. Immunol.*, 2006, **177**, 4679.
11 T. Jouault, A. Sarazin, M. Martinez-Esparza, C. Fradin, B. Sendid and D. Poulain, *Cell. Microbiol.*, 2009, **11**, 1007.
12 S. G. Filler, *Curr. Opin. Microbiol.*, 2006, **9**, 333.
13 S. M. Levitz, *PLoS Pathog.*, 2010, **6**, e1000758.
14 L. Kohatsu, D. K. Hsu, A. G. Jegalian, F. T. Liu and L. G. Baum, *J. Immunol.*, 2006, **177**, 4718.
15 G. D. Brown and S. Gordon, *Nature*, 2001, **413**, 36.
16 G. D. Brown, J. Herre, D. L. Williams, J. A. Willment, A. S. Marshall and S. Gordon, *J. Exp. Med.*, 2003, **197**, 1119.
17 S. C. Cheng, F. L. van de Veerdonk, M. Lenardon, M. Stoffels, T. Plantinga, S. Smeekens, L. Rizzetto, L. Mukaremera, K. Preechasuth, D. Cavalieri, T. D. Kanneganti, J. W. van der Meer, B. J. Kullberg, L. A. Joosten, N. A. Gow and M. G. Netea, *J. Leukocyte Biol.*, 2011, **90**, 357.
18 N. R. Cohen, R. V. Tatituri, A. Rivera, G. F. Watts, E. Y. Kim, A. Chiba, B. B. Fuchs, E. Mylonakis, G. S. Besra, S. M. Levitz, M. Brigl and M. B. Brenner, *Cell Host Microbe*, 2011, **10**, 437.
19 H. L. Cash, C. V. Whitham, C. L. Behrendt and L. V. Hooper, *Science*, 2006, **313**, 1126.
20 A. Schlosser, T. Thomsen, J. B. Moeller, O. Nielsen, I. Tornoe, J. Mollenhauer, S. K. Moestrup and U. Holmskov, *J. Immunol.*, 2009, **183**, 3800.
21 H. M. Mora-Montes, M. G. Netea, G. Ferwerda, M. D. Lenardon, G. D. Brown, A. R. Mistry, B. J. Kullberg, C. A. O'Callaghan, C. C. Sheth, F. C. Odds, A. J. Brown, C. A. Munro and N. A. Gow, *Infect. Immun.*, 2011, **79**, 1961.
22 N. Shibata, A. Suzuki, H. Kobayashi and Y. Okawa, *Biochem. J.*, 2007, **404**, 365.
23 H. Kobayashi, N. Shibata, M. Nakada, S. Chaki, K. Mizugami, Y. Ohkubo and S. Suzuki, *Arch. Biochem. Biophys.*, 1990, **278**, 195.
24 P. W. de Groot, E. A. Kraneveld, Q. Y. Yin, H. L. Dekker, U. Gross, W. Crielaard, C. G. de Koster, O. Bader, F. M. Klis and M. Weig, *Eukaryotic Cell*, 2008, **7**, 1951.
25 Y. F. Dufrêne, *Nat. Protoc.*, 2008, **3**, 1132.
26 D. J. Muller and Y. F. Dufrene, *Nat. Nanotechnol.*, 2008, **3**, 261.
27 D. J. Müller and Y. F. Dufrêne, *Curr. Biol.*, 2011, **21**, R212.
28 D. Poulain, J. C. Cailliez and J. F. Dubremetz, *Eur. J. Cell Biol.*, 1989, **50**, 94.
29 M. Martinez-Esparza, A. Sarazin, D. Poulain and T. Jouault, *Methods Mol. Biol.*, 2009, **470**, 85.
30 F. Dalle, T. Jouault, P. A. Trinel, J. Esnault, J. M. Mallet, P. d'Athis, D. Poulain and A. Bonnin, *Infect. Immun.*, 2003, **71**, 7061.
31 P. A. Trinel, G. Lepage, T. Jouault, G. Strecker and D. Poulain, *FEBS Lett.*, 1997, **416**, 203.
32 D. Alsteens, M. C. Garcia, P. N. Lipke and Y. F. Dufrene, *Proc. Natl. Acad. Sci. U. S. A.*, 2010, **107**, 20744.
33 A. B. van Spriel and C. G. Figdor, *Microbes Infect.*, 2010, **12**, 106.
34 G. Francius, S. Lebeer, D. Alsteens, L. Wildling, H. J. Gruber, P. Hols, S. De Keersmaecker, J. Vanderleyden and Y. F. Dufrene, *ACS Nano*, 2008, **2**, 1921.
35 M. Harris, H. M. Mora-Montes, N. A. Gow and P. J. Coote, *Microbiology*, 2009, **155**, 1058.
36 H. M. Mora-Montes, S. Bates, M. G. Netea, L. Castillo, A. Brand, E. T. Buurman, D. F. Diaz-Jimenez, B. Jan Kullberg, A. J. Brown, F. C. Odds and N. A. Gow, *J. Biol. Chem.*, 2010, **285**, 12087.
37 G. D. Brown, *Nat. Rev. Immunol.*, 2006, **6**, 33.
38 B. Ferwerda, G. Ferwerda, T. S. Plantinga, J. A. Willment, A. B. van Spriel, H. Venselaar, C. C. Elbers, M. D. Johnson, A. Cambi, C. Huysamen, L. Jacobs, T. Jansen, K. Verheijen, L. Masthoff, S. A. Morre, G. Vriend, D. L. Williams, J. R. Perfect, L. A. Joosten, C. Wijmenga, J. W. van der Meer, G. J. Adema, B. J. Kullberg, G. D. Brown and M. G. Netea, *N. Engl. J. Med.*, 2009, **361**, 1760.
39 P. R. Taylor, S. V. Tsoni, J. A. Willment, K. M. Dennehy, M. Rosas, H. Findon, K. Haynes, C. Steele, M. Botto, S. Gordon and G. D. Brown, *Nat. Immunol.*, 2007, **8**, 31.
40 O. Gross, A. Gewies, K. Finger, M. Schafer, T. Sparwasser, C. Peschel, I. Forster and J. Ruland, *Nature*, 2006, **442**, 651.

41 B. N. Gantner, R. M. Simmons and D. M. Underhill, *EMBO J.*, 2005, **24**, 1277.
42 C. Fradin, T. Jouault, A. Mallet, J. M. Mallet, D. Camus, P. Sinay and D. Poulain, *J. Leukocyte Biol.*, 1996, **60**, 81.
43 M. Lienemann, A. Paananen, H. Boer, J. M. de la Fuente, I. Garcia, S. Penades and A. Koivula, *Glycobiology*, 2009, **19**, 633.
44 G. Lesage and H. Bussey, *Microbiol. Mol. Biol. Rev.*, 2006, **70**, 317.
45 C. A. Munro, K. Winter, A. Buchan, K. Henry, J. M. Becker, A. J. Brown, C. E. Bulawa and N. A. Gow, *Mol. Microbiol.*, 2001, **39**, 1414.
46 G. Marquis, S. Garzon, S. Montplaisir, H. Strykowski and N. Benhamou, *J. Leukocyte. Biol.*, 1991, **50**, 587.
47 S. Kasas and A. Ikai, *Biophys. J.*, 1995, **68**, 1678.
48 A. Ebner, L. Wildling, A. S. M. Kamruzzahan, C. Rankl, J. Wruss, C. D. Hahn, M. Hölzl, R. Zhu, F. Kienberger, D. Blaas, P. Hinterdorfer and H. J. Gruber, *Bioconjugate Chem.*, 2007, **18**, 1176–1184.